Supplement of Atmos. Meas. Tech., 13, 4247–4259, 2020
https://doi.org/10.5194/amt-13-4247-2020-supplement

Atmospheric Measurement Techniques
Open Access
EGU

Supplement of

A new TROPOMI product for tropospheric NO_2 columns over East Asia with explicit aerosol corrections

Mengyao Liu et al.

Correspondence to: Jintai Lin (linjt@pku.edu.cn)

This PDF file includes 10 pages containing

1. MAX-DOAS instruments
2. Evaluation of sampling consistency between TROPOMI and MAX-DOAS data
3. Tables S1 to S3
4. Figures S1 and S2
5. SI references

Part A. MAX-DOAS instruments

The instrument in Nanjing is a mini MAX-DOAS with Maya2000Pro (Ocean Optics, Dunedin, FL, USA) spectrometer, which is on the roof of the School of Atmospheric Science in the Xianlin Campus of Nanjing University, about 17.7 km northeast of Nanjing urban center. The controlled temperature is set at 20℃ for all seasonas. It measures scattered sunlight every 15 min at eleven elevation angles: 1°, 2°, 3°, 4°, 5°, 6°, 8°,10°, 20°, 30°, and 90°. The instruments were normally operated from 8:00 to 17:00 local time (LT) each day. The details can be found in Tian et al.,(2018).

The instrument in Xuzhou is a MAX-DOAS 2000 located on the roof of the School of Environmental Science and Spatial Informatics, China University of Mining and Technology, 6.5 km away from Xuzhou urban center. This site is about 1 km south of Yulong Lake Scenic Area, an AAAAA (5A) scenic area with mountains and lakes. The instrument measures scattered sunlight every 5 minutes at five elevation angles: 5°, 10°, 20°, 30°, and 90°.

The remote Fukue site is away from major cities (e.g., 100 km from Nagasaki, a city with 440,000 residents). The miniature spectrometer used here is USB4000 (Ocean Optics, Dunedin, FL, USA). A prism is rotated every 5 min to introduce scattered sunlight from the sky, with sequential elevation angles of the telescope at 3°, 5°, 10°, 20°, 30°, and 90°. One cycle of observations at six elevation angles (with 5 min integration each) takes 30 min (Kanaya et al., 2014).

Part B. Evaluation of sampling consistency between TROPOMI and MAX-DOAS data

When comparing satellite products and MAX-DOAS observations, ensuring temporal and spatial sampling consistencies is crucial. Figure 3 shows the spatial distributions of POMINO-TROPOMI NO_2 VCDs around two suburban sites, Nanjing and Xuzhou sites. The spatial distribution around Xuzhou site is much smoother than Nanjing.

Tables S4 and S5 present the statistical results of satellite data evaluation at Xuzhou and Nanjing, by varying the distance between a TROPOMI pixel center and a MAX-DOAS site and by varying the time difference between the MAX-DOAS measurement and TROPOMI overpass. A similar analysis is not done for Fukue because of too few data points (i.e., five days in total for a sensitivity study).

Tables S2 and S3 show that the R^2 varies (between 0.33 and 0.91) with the sampling distance and time. Extending the sampling time or expanding the sampling distance tends to decrease the R^2, reflecting the decreasing sampling consistency. However, extending the sampling time from within $\pm$0.5 hours to within $\pm$1 hours decreases the normalized mean bias. Based on these comparison results, we choose within 5 km and within $\pm$1 h (similar to Liu et al. (2019)) as our sampling choice in the main text.

Table S1. Retrieval parameters used for NO_2 VCD retrievals.

Product	**POMINO-TROPOMI**	**TM5-MP-DOMINO**	**POMINO v2 for the OMI instrument**
RTM	LIDORT v3.6 (un-polarized, curved atmosphere)	DAK v3.2 (pseudo-sphericity and polarization correction)	LIDORT v3.6 (un-polarized, curved atmosphere);
Calculation for individual pixels	Pixel-specific radiative transfer modeling; no LUT	LUT	Pixel-specific radiative transfer modeling; no LUT
Surface reflectance	MCD43C2 Collection 6 (0.05°) BRDF at 440 nm over lands and OMLER v3 albedo over open oceans	Lambertian surface albedo; 5-year climatology data (0.5°), see Kleipool et al. (2008)	MCD43C2 Collection 6 (0.05°) BRDF at 440 nm over lands and OMLER v3 albedo over open oceans
Surface pressure	GEOS-FP[a], adjusted by elevation[b]	TM5-MP v3 model, adjusted by elevation[c]	GEOS-FP[a] since May 2013 and GEOS-5[a] before May 2013, adjusted by elevation[b]
Aerosol optical parameters	GEOS-Chem v9-02[a]; at 437.5 nm; model AOD is adjusted by MODIS/Aqua C6.1 AOD[d]	N/A	GEOS-Chem v9-02[a], at 439 nm; model daily AOD is adjusted by monthly MODIS/Aqua C6.1 AOD[d]; model daily aerosol shape is corrected by a monthly CALIOP climatology over 2007-2015[d]
Cloud fraction and cloud pressure	Cloud pressure is from FRESCO-S at O_2 A-band (758 nm); cloud fraction is derived in this study at the NO_2 fitting window (at 437.5 nm)[e]; Pixel-specific RTM calculations for cloud fractions with no LUT	Cloud pressure is from FRESCO-S at O_2 A-band (758 nm); cloud fraction is derived at the NO_2 fit window (at 437.5 nm)[e]; LUT for cloud fractions	Both are derived at O_2-O_2 band (at 475nm)[f]; Pixel-specific RTM calculations with no LUT
Vertical profile of NO_2	GEOS-Chem v9-02[a]	TM5-MP v3 model[c]	GEOS-Chem v9-02[a]
Vertical profiles of pressure and temperature	GEOS-FP[a]	TM5-MP v3 model[c]	GEOS-FP[a] since May 2013 and GEOS-5[a] before May 2013
Reference	This study	Arnoud et al., (2019); van Geffen et al., (2019)	J.T. Lin et al. (2014); J.T. Lin et al. (2015); Liu et al. (2019)

[a] GEOS-FP and GEOS-5 are assimilated meteorological fields used to drive GEOS-Chem v9-02 simulations. The GEOS-Chem model and meteorological fields have the same spatial resolutions, horizontally and vertically. GEOS-FP and GEOS-5 meteorological fields are horizontally gridded at 0.25° lat. × 0.3125° long. and 0.5° lat. × 0.667° long., respectively. Both meteorological fields have 47 layers vertically, with ~ 10 layers below 1.5 km.

[b] Elevation information is from the GMTED2010 data set at 30 arcsec (http://topotools.cr.usgs.gov/GMTED_viewer/). The pressure levels are re-calculated according to the elevation-adjusted surface pressure, while the volume mixing ratios of NO_2 are not changed in individual layers (Zhou et al., 2010).
[c] Pixel-averaged terrain height based on a 3-km resolution digital elevation map (Maasakkers et al., 2013). The pressure levels are corrected based on the method described in Zhou et al. (2010) and Boersma et al. (2011). Vertical NO_2 profiles are simulated at 1° long. × 1° lat. with 34 layers vertically in the TM5-MP v3 model driven by ECMWF meteorological data.
[d] See Lin et al. (2014, 2015) for AOD correction and see Liu et al. (2019) for the adjustment of the aerosol vertical shapes.
[e] The cloud retrievals of POMINO-TROPOMI and TM5-MP-DOMINO (OFFLINE) follow the methodology described by Arnoud et al. (2017) and van Geffen et al. (2019) TM5-MP-DOMINO (OFFLINE) compiled a LUT of the reflectance at TOA at the NO_2 fitting window for the cloud fraction retrieval. POMINO-TROPOMI calculates the cloud fraction for each pixel online.
[f] See Lin et al. (2014) and Liu et al. (2019) for details.

Table S2 Statistical results of RMA as a function of sampling distances and times at Xuzhou.

Within ± 0.5 h	5 km	15 km	25 km
R^2	0.49	0.40	0.33
Slope	0.65	0.57	0.51
Intercept (10^{15} molec·cm^{-2})	3.02	3.59	3.65
NMB (%)	−10.1	−12.8	−20.2
Number [1]	34	41	43
Within ± 1 h	5 km	15 km	25 km
R^2	0.63	0.48	0.44
Slope	0.80	0.69	0.60
Intercept (10^{15} molec·cm^{-2})	1.40	2.30	3.0
NMB (%)	−5.6	−7.6	−14.4
Number [1]	28	34	34

[1] The fewer number of valid days when the (temporal) sampling window is expanded is because of increased temporal variability to the extent that violates our data selection criterion (standard deviation < 20% of the mean in MAX-DOAS data).

Table S3 Statistical results of RMA as a function of sampling distances and times at Nanjing.

Within ± 0.5 h	5 km	15 km	25 km
R^2	0.91	0.73	0.70
Slope	0.63	0.65	0.57
Intercept (10^{15} molec·cm^{-2})	1.42	2.21	2.76
NMB (%)	−22.6	−15.3	−19.4
Number	13	21	22
Within ± 1 h	5 km	15 km	25 km
R^2	0.77	0.35	0.40
Slope	0.60	0.93	0.71
Intercept (10^{15} molec·cm^{-2})	2.31	−2.30	1.19
NMB (%)	−12.3	−1.5	−5.4
Number	21	28	30

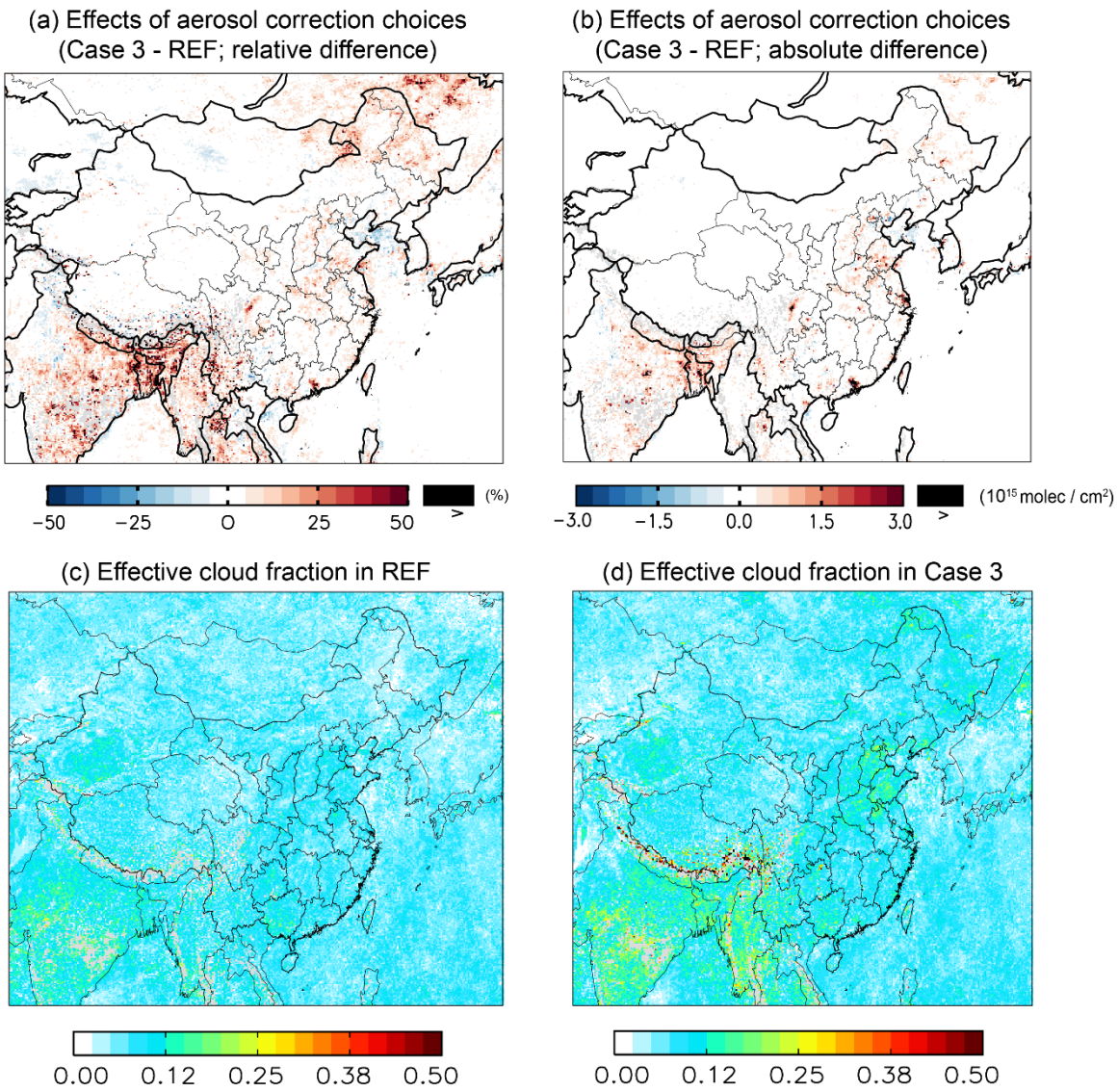

Figure S1. (a) Relative and (b) absolute differences in retrieved NO_2 VCDs in July 2018 between using "semi-explicit" aerosol corrections and using explicit aerosol corrections (Case 3 – REF). (c) – (d) are the effective cloud fractions in Case REF and Case 3.

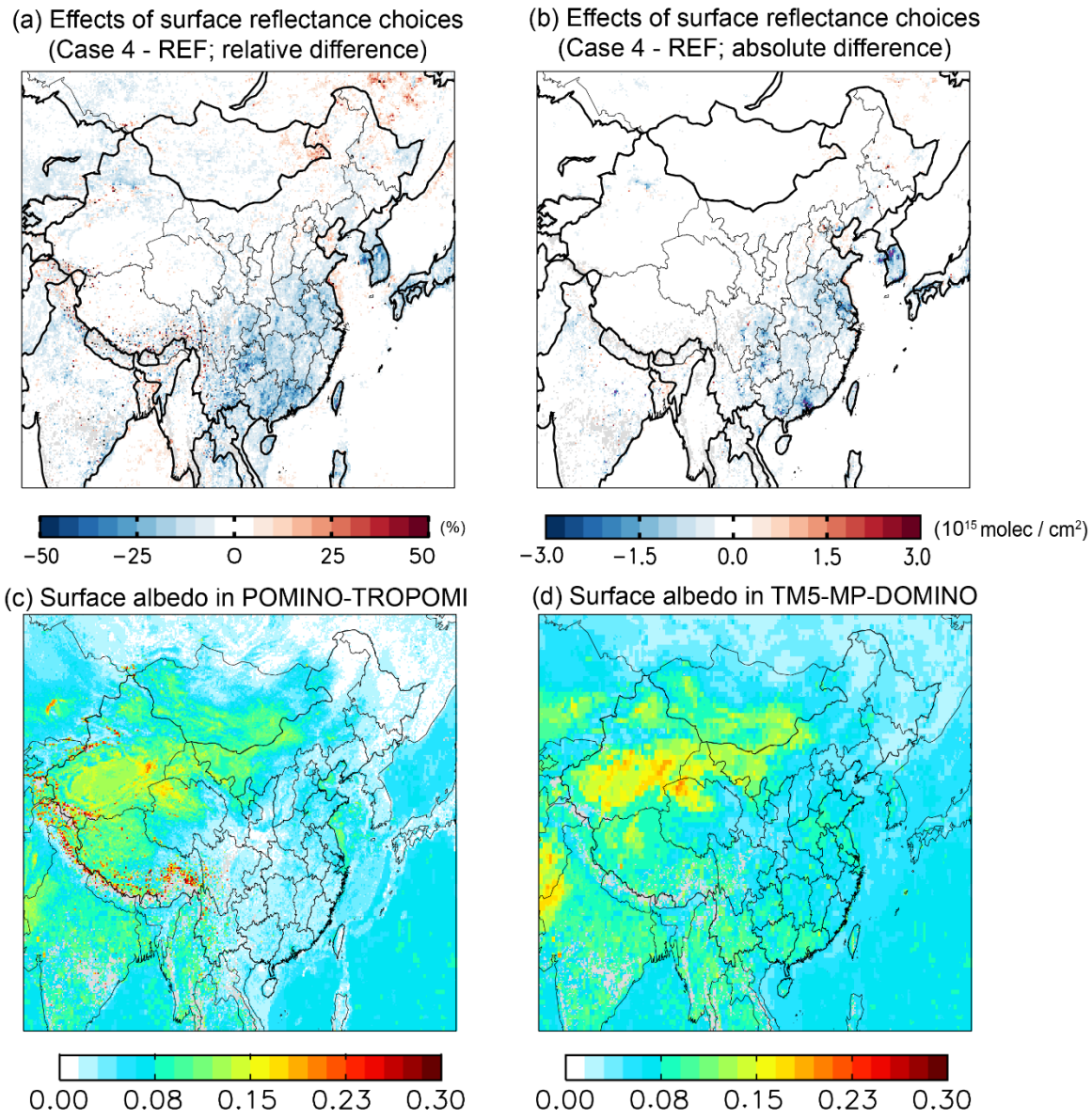

Figure S2. (a) Relative and (b) absolute differences in retrieved NO_2 VCDs in July 2018 between using MODIS BRDF and using OMI LER (Case 4 – REF). (c) – (d) are the blue-sky albedos in Case REF (derived from MODIS BRDF) and the LER albedos in Case 4.

References:

Arnoud, A., Mattia, P., Maarten, S., Veefkind, J. P., Loyola, D., & Wang, P. (2017). *Sentinel-5 precursor/TROPOMI Level 2 Product User Manual KNMI level 2 support products*. Retrieved from De Bilt, the Netherlands: https://sentinel.esa.int/documents/247904/2474726/Sentinel-5P-Level-2-Product-User-Manual-FRESCO-Cloud-Support

Boersma, K. F., Eskes, H. J., Dirksen, R. J., van der A, R. J., Veefkind, J. P., Stammes, P., Brunner, D. (2011). An improved tropospheric NO_2 column retrieval algorithm for the Ozone Monitoring Instrument. *Atmos. Meas. Tech., 4*(9), 1905-1928. doi:10.5194/amt-4-1905-2011

Kanaya, Y., Irie, H., Takashima, H., Iwabuchi, H., Akimoto, H., Sudo, K., Panchenko, M. (2014). Long-term MAX-DOAS network observations of NO_2 in Russia and Asia (MADRAS) during the period 2007-2012: instrumentation, elucidation of climatology, and comparisons with OMI satellite observations and global model simulations. *Atmos. Chem. Phys., 14*(15), 7909-7927. doi:10.5194/acp-14-7909-2014

Kleipool, Q. L., Dobber, M. R., De Haan, J. F., and Levelt, P. F. (2008). Earth surface reflectance climatology from 3 years of OMI data. J. Geophys. Res., 113(D18308):22 pp

Lin, J. T., Martin, R. V., Boersma, K. F., Sneep, M., Stammes, P., Spurr, R., Irie, H. (2014). Retrieving tropospheric nitrogen dioxide from the Ozone Monitoring Instrument: effects of aerosols, surface reflectance anisotropy, and vertical profile of nitrogen dioxide. *Atmos. Chem. Phys., 14*(3), 1441-1461. doi:10.5194/acp-14-1441-2014

Lin, J. T., Liu, M. Y., Xin, J. Y., Boersma, K. F., Spurr, R., Martin, R., & Zhang, Q. (2015). Influence of aerosols and surface reflectance on satellite NO_2 retrieval: seasonal and spatial characteristics and implications for NO_x emission constraints. *Atmos. Chem. Phys., 15*(19), 11217-11241. doi:10.5194/acp-15-11217-2015

Liu, M., Lin, J., Boersma, K. F., Pinardi, G., Wang, Y., Chimot, J., Ni, R. (2019). Improved aerosol correction for OMI tropospheric NO_2 retrieval over East Asia: constraint from CALIOP aerosol vertical profile. *Atmos. Meas. Tech., 12*(1), 1-21. doi:10.5194/amt-12-1-2019

Maasakkers, J. D., K. F. Boersma, J. E. Williams, J. Van Geffen, G. C. M. Vinken, M. Sneep, F. Hendrick, M. Van Roozendael, and J. P. Veefkind (2013), Vital improvements to the retrieval of tropospheric NO2 columns from the Ozone Monitoring Instrument, in EGU General Assembly 2013, edited, pp. EGU2013-2714, EGU General Assembly Conference Abstracts.

Tian, X.; Gao, Z. Validation and Accuracy Assessment of MODIS C6.1 Aerosol Products over the Heavy Aerosol Loading Area. Atmosphere 2019, 10(9), 548, https://doi.org/10.3390/atmos10090548

van Geffen, J. H. G. M., Eskes, H. J., Boersma, K. F., Maasakkers, J. D., & Veefkind, J. P. (2019). *TROPOMI ATBD of the total and tropospheric NO_2 data products (issue 1.4.0)*. Retrieved from De Bilt, the Netherlands: https://sentinel.esa.int/documents/247904/2476257/Sentinel-5P-TROPOMI-ATBD-NO2-data-products

Zhou, Y., D. Brunner, R. J. D. Spurr, K. F. Boersma, M. Sneep, C. Popp, and B. Buchmann (2010), Accounting for surface reflectance anisotropy in satellite retrievals of tropospheric NO_2, Atmos. Meas. Tech., 3(5), 1185-1203.